Numerical Ages of Selected Rudist Bivalvia: Preliminary Results

ROBERT W. SCOTT

Precision Stratigraphy Associates and University of Tulsa, 149 West Ridge Road,
Cleveland, Oklahoma 74020, USA (E-mail: rwscott@cimtel.net)

Abstract: The ranges of most biostratigraphically diagnostic fossils have been calibrated to the geologic time scale in mega-annums. Five methods for integrating fossil ranges with the numerical geologic time scale are currently used: (1) species in stratigraphic positions with radiometrically dated beds; (2) strontium isotopes of unaltered shell material; (3) cyclostratigraphic frequencies of enclosing strata; (4) integration with zones and sequence stratigraphy; and (5) graphic correlation.

Preliminary studies show that rudist occurrences have been calibrated in numerical ages by Sr isotopes, zonal integration and graphic correlation. Where the same species are dated by two methods, a more complete range is the result. The different methods not only complement each other, but also test each other. This preliminary survey demonstrates the feasibility of compiling an extensive stratigraphic database of each species and calibrating the numerical ranges in each section in order to define the maximum ages and the region of origins of rudist species.

Key Words: Rudists, numerical ages, graphic correlation, strontium isotopes

Seçilmiş Rudist Bivbialiaların Sayısal Yaşı: Ön Sonuçlar

Özet: Biyostratigrafik açıdan karakteristik fosillerin çoğunun düşey dağılımları mega-annums'da jeolojik zaman çizelgesi ile kalibre edilmiştir. Bugün, fosil düşey dağılımları ile sayısal jeolojik zaman çizelgesinin entegre edildiği beş yöntem kullanılmaktadır: (1) radyometrik olarak yaşlandırılmış katmanlardaki türlerin stratigrafik konumları; (2) altere olmamış kavkı malzemesinin stronsiyum izotopları; (3) katmanların siklostratigrafik frekansları; (4) zonlar ile sekans stratigrafisinin entegrasyonu; ve (5) grafik korelasyon.

Ön çalışmalar, rudistlerin Sr izotoplar, zonal entegrasyon ve grafik korelasyonla elde edilen sayısal yaşlar ile kalibre edildiklerini göstermektedir. Aynı tür iki yöntemle yaşlandırıldığında, daha sağlıklı bir düşey dağılım elde edilir. Farklı yöntemler sadece birbirini desteklemekle kalmaz aynı zamanda birbirini kontrol da eder. Bu ilk çalışmalar, rudist türlerinin maksimum yaşlarının ve ortaya çıkış bölgelerinin saptanması amacıyla her bir tür için geniş bir stratigrafik veritabanı oluşturmanın ve her kesitte sayısal yaşları kalibre etmenin mümkün olduğunu göstermektedir.

Anahtar Sözcükler: Rudistler, sayısal yaşlar, grafik korelasyon, stronsiyum izotopları

Introduction

A major goal of chronostratigraphy is the calibration of fossil ranges in terms of numerical ages in mega-annums (Ma). With new methodologies such as strontium isotopes and cyclostratigraphy this goal seems attainable. Indeed, numerous recent publications present ages of first (FO) and last occurrences (LO) of many biostratigraphically important fossil species (Berggren *et al.* 1995; Hardenbol *et al.* 1998; Gradstein *et al.* 2004). This paper is a preliminary summary of ages of rudist Bivalvia. It presents a vision of what is possible although the current data are limited by sparse sampling and limited databases. This first tabulation of rudist ages is designed to promote future studies towards this goal.

Presently three methods have been applied to interpolate numerical ages of rudist occurrences. The knowledge of rudist specialists was the basis for integrating rudist ranges with other fossils in the important summary by Hardenbol *et al.* (1998). Secondly, Sr isotopes of unaltered rudist shells have been plotted on the standard Sr^{86}/Sr^{87} curve for the Cretaceous (Steuber *et al.* 2007). Thirdly, rudist occurrences in published measured sections in the Tethyan Realm where other biostratigraphic species are present (Figure 1, Appendix 1) were incorporated into a large integrated database by graphic correlation (Scott 2009). These methods are reviewed as related to rudist ranges and the existing numerical ages are compared. This review suggests that rudist occurrences can be accurately calibrated to numerical time scales given adequate data.

Methods, Materials Studied

Strontium Isotopes

Secular changes in seawater composition of Mg, Ca, and Sr are well documented (summarized by Steuber & Rauch 2005). The changing ratio of strontium isotopes through the Phanerozoic is calibrated to stages and zones (McArthur & Howarth 2004). The current geologic time scale of the stages is projected into this curve. The Sr isotope ratio of a given sample is then projected back into the time scale. This process provides a quantitative method to calibrate numerical ages of first and last species occurrences. The curve through the Cretaceous is well constrained and has a number of long-term gradients (Bralower *et al.* 1997; McArthur *et al.* 2001; Steuber 2002). However the curve is rather flat during the Barremian and the Albian–Cenomanian so that accurate ages cannot be interpolated during this time span. The Sr-isotope scale has been used to date a number of rudist species because the unaltered calcite comprising the outer shell layer of many rudists retains the original ratio (Steuber 2001, 2003; Steuber *et al.* 2002; Steuber & Rauch 2005). The mean age or the maximum and minimum ages are given for species where a range was published (Table 1).

A cautionary issue is that rudist occurrences in specific sections may not record their oldest appearance or their youngest age at the time of
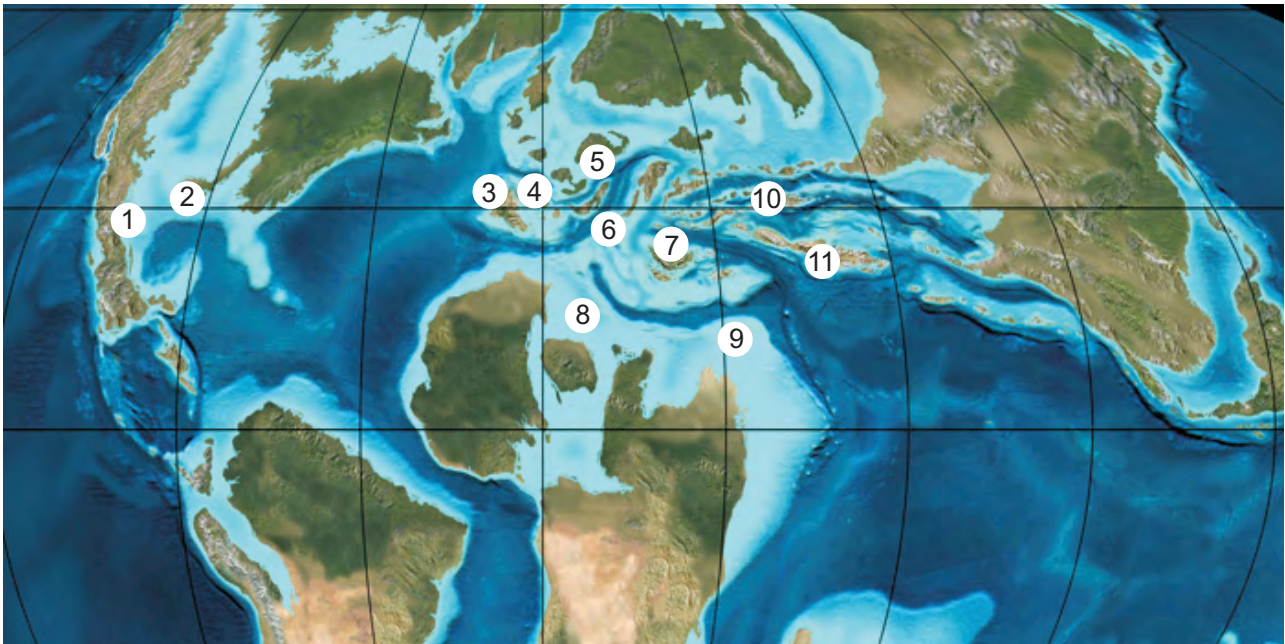

Figure 1. Location of measured sections containing rudists. Numbered sites indicate positions of section groups as numbered in Appendix 1. Base map is Mollewide Projection at 90 Ma from R.C. Blakey, University of Northern Arizona (with permission) (http://jan.ucc.nau.edu/~rcb7/ globaltext2.html).

Table 1. Ages of selected rudist species by graphic correlation, strontium isotopes, and zonal integration (by Masse and Philip in Hardenbol *et al.* 1998, Chart 5) compared. Sources of Sr isotope ages: 1– Steuber *et al.* (2007); 2– Steuber *et al.* (1998); 3– Steuber (2001); 4– Steuber *et al.* (2002).

Taxa	MIDK45		Strontium		1998 Stages	
	FO	LO	FO	LO	FO	LO
Family Requieniidae						
Apricardia carentonensis	95.98	93.13				
Apricardia laevigata	95.98	93.13				
Pseudotoucasia santanderensis	114.91	113.71			116.09	
Toucasia patagiata	105.53	105.49				
Toucasia texana	105.21	103.92				
Family Caprinidae						
Caprina choffati	99.19	98.86			103.18	
Caprina douvillei	122.03	120.72			120.49	117.56
Caprina gracilis	105.47	101.81				
Caprinula boissyi	93.45	93.17				93.49
Caprinula brevis	93.45	93.17				
Caprinula d'orbignyi	93.45	93.17				
Caprinula doublieri	93.45	93.17				
Offneria sp.	122.7	120.72			120.98	117.07
Orthopthychus striatus	95.95	94.22				
Pachytraga paradoxa	122.03	120.72			121.74	117.56
Schiosia carinatoformis	95.95	94.22			96.93	
Caprinuloidea multitubifera	105.81	104.61				
Caprinuloidea perfecta	107.43	103.92				
Coalcomana ramosa	112.01	108.19				
Kimbleia albrittoni	100.23	97.91				
Kimbleia capacis	100.27	98.23				
Mexicaprina alata	98.09	97.97				
Mexicaprina cornuta	99.64	99.14				
Mexicaprina minuta	98.75	97.91				
Mexicaprina quadrata	98.14	97.91				
Texicaprina vivari	107.37	100.29				
Family Monopleuridae						
Monopleura marcida	111.69	105.49				
Glossomyophorus sp.	122.99	122.42				
"Petalodontia" calamitiformis	106.82	104.04				
Family Radiolitidae						
Agriopleura darderi	110.86	108.67			113.16	101.06
Agriopleura falconi[4]			65.83	65.83		
Biradiolites angulosus	90.32	89.99				
Biradiolites chaperi[1]			66.4±0.5	66.4±0.5		
Biradiolites jamaicensis[4]			65.83	65.83		
Biradiolites minhoensis[4]			66.68	65.78		
Biradiolites rudis[4]			66.68	65.78		
Biradiolites rudissimus[4]			66.68	65.78		
Bournonia barretti[4]			66.68	65.78		
Bournonia cancellata[4]			66.68	65.78		
Bournonia fourtaui	90.32	89.99				
Bournonia judaica	88.95	88.95				
Bournonia subcancellata[4]			66.68	65.78		
Bournonia tetrahedron[4]			66.68	65.78		
Chiapsella radiolitiformis[4]			66.68	65.78		
Distefanella lombricalis	90.32	89.99				
Distefanella mooretownensis[4]			69.12	69.05		
Durania arnaudi	93.45	91.25			92.69	
Durania austinensis	82.53	82.27				
Durania cornupastoris	91.9	91.64				88.96
Durania gaensis	90.32	89.99				
Durania nicholasi[4]			66.68	65.78		
Eoradiolites davidsoni	106.86	97.91				
Eoradiolites lyratus	104.24	93.74			106.35	
Joufia reticulata[1]			66.8	65.5		

771

Table 1. Contunied.

Taxa	MIDK45		Strontium		1998 Stages	
	FO	LO	FO	LO	FO	LO
Pseudopolyconites apuliensis[1]			66.4±0.5	66.4±0.5		
Praeradiolites biskraensis	93.96	93.96				
Praeradiolites fleuriaui	91.63	91.63				
Praeradiolites irregularis	91.75	92.51				
Radiolites lusitanicus	93.23	93.06				93.49
Radiolites peroni	93.06	93.06				
Radiolites sauvagesi	90.32	89.99				
Radiotella maestichtiana[1]			66.4±0.5	66.4±0.5		
Sauvagesia acutocostata	82.53	82.27				
Sauvageisa macroplicata[4]			66.68	65.78		
Sauvageisa mcgrathi[4]			66.68	65.78		
Sauvagesia sharpei						93.49
Thyrastylon coryi[4]			66.68	65.78		
Thyrastylon semiannulosus[4]			66.68	65.78		
Family Hippuritidae						
Hippurites cornicopiae[1]			66.8	65.5	67.78	
Hippurites requieni	92.7	89.99			91.88	
Hippuritella lapeirousei[1]			66.8	65.5		65.53
Orbignya mullerriedi[4]			66.68	65.78		
Pironaea polystyla[1]			66.8	65.5		
Praebarrettia sparcilrata[4]			66.68	65.78		
Vaccinites alpinus[3]			83.88	83.88		
Vaccinites boehmi[3]			87.21	87.21	83.46	
Vaccinites cornuvaccinum[3]			87.33	86.87		
Vaccinites gosaviensis[3]			83.97	83.97	85.79	
Vaccinites inaequicostatus[3]			89.75	87.92		
Vaccinites praegiganteus	91.47	91.14			90.36	
Vaccinites ultimus[2,3]			82-81	80.13	72.71	
Yvaniella alpani[2]			82-81	82-81		
Family Polyconitidae						
Polyconites verneuilli	115.57	112.06			116.09	
Horiopleura baylei	120.61	116.34				
Horiopleura lamberti	115.57	112.06			115.11	100.53
Family Plagioptychidae						
Mitrocaprina bulgarica[1]			66.4±0.5	66.4±0.5		
Mitrocaprina multicaniculata[4]			66.68	65.78		
Plagioptychus fragilis[4]			65.83	65.83		
Plagioptychus jamaicensis[4]			66.68	65.78		
Plagioptychus minor[4]			66.68	65.78		
Plagioptychus trechmanni[4]			66.68	65.78		
Plagioptychus zansi[4]			65.83	65.83		
Family Ichthyosarcolitidae						
Ichthyosarcolites bicarinatus	95.95	94.22			96.93	
Ichthyosarcolites poljaki	95.95	94.22				
Ichthyosarcolites tricarinatus	95.95	94.22			96.93	
Titanosarcolites giganteus[4]	69.12	65.78				
Family Antillocaprinidae						
Antillocaprina occidentalis[4]			66.68	65.78		
Antillocaprina suboccidentalis[4]			66.68	65.78		

1– Steuber *et al.* 2007; 2– Steuber *et al.* 1998; 3– Steuber 2001; 4– Steuber *et al.* 2002; 5– Sarı *et al.* 2004

extinction. The Sr method is best applied to rudist groups having thick calcite shell layers. However some groups, such as Caprinuloidea, secreted a very thin calcite layer and the thicker aragonite layer normally is altered to calcite spar. Thus the method cannot be applied to significant sets of species.

Zonal Integration

The numerical ages of a number of rudist species were reported by Jean-Pierre Masse and Jean Philip (in Hardenbol *et al.* 1998, chart 5). The ages of species in common with the graphic correlation database are expressed to the second decimal position signifying a precision of tens of thousand years (Table 1); many other species are not included here. The ranges of these species are based on the many years of experience of these specialists. The ages are interpolated by relating rudist occurrences to standard zones and stage boundaries and sequence boundaries, which have been calibrated to the current time scale. The actual sections and range measurements, however, were not published. Thus, the accuracy of these ages cannot be evaluated and the range data cannot be tested except by an independent study of measured sections.

Graphic Correlation

An alternative method of interpolating numerical ages to the ranges of rudists or any other fossil is by Graphic Correlation. Graphic correlation is a quantitative, non-statistical, technique that determines the coeval relationships between two sections by comparing the ranges of event records in both sections (Carney & Pierce 1995). A graph of any pair of sections is an X/Y plot of the FOs (bases) and LOs (tops) of taxa found in both sections. The interpreter places a line of correlation (LOC) through the tops and bases that are at their maximum range in both sections. This LOC is the most constrained hypothesis of synchroneity between the two sections and alters the fewest bioevents. The LOC also accounts for hiatuses or faults at stratal discontinuities indicated by the lithostratigraphic record. The position of the LOC is defined by the equation for a regression line. Explanation and examples of the graphic technique

are illustrated by Miller (1977) and Carney & Pierce (1995). By graphing successive sections a database of ranges is compiled. The result of this iterative graphing process is a database of sections in which the species occurs and the oldest and youngest occurrences of a species. The accuracy of these ranges depends on the number of sections, preservation and correct identification of the species. Such a database is testable and the process is transparent so that the fossil occurrence in each section can be evaluated to determine its accuracy. This process compiles data of many specialists who have studied many sections.

The original method of graphic correlation compared the spacing of events in terms of thickness of the SRS (Carney & Pierce 1995). A refined method is to graph the SRS to a time scale so that the events are directly projected into numerical ages. The compilation of the MIDK45 database began with construction of the MIDK3 database in which the first step was to graph the Cenomanian–Turonian section at Kalaat Senan, Tunisia, to the 1989 time scale (Harland *et al.* 1990; Scott *et al.* 2000). The sedimentology, sequence stratigraphy, and biostratigraphy of the Tunisian section were carefully documented and the section recorded continuous deposition at a uniform rate (Robaszynski *et al.* 1990, 1993). The stage boundaries were clearly defined by the ranges of key fossils so that the LOC could be pinned to them. Thus all events were related to time. To further constrain the numeric ages of the database scale, sections with radiometrically dated beds were graphed and the X-axis scale was re-calibrated to millions of years (mega-annum, Ma) (Carney & Pierce 1995; Scott *et al.* 2000; Scott 2009).

The new method of graphic correlation results in the comprehensive MIDK45 database that avoids the limitations of the method noted by Gradstein *et al.* (2004). The ranges of more than 3000 bioevents and other markers in nearly 200 measured sections are calculated instantaneously and used in the interpretation of each subsequent section. The MIDK45 database evolved in successive steps from the MIDK3, MIDK4, MIDK41, and MIDK42 Chronostratigraphic Databases. The latter data set was compiled for the CORB Cretaceous time scale from published reports of 150 outcrops and cored

sections, by adding 40 additional sections (Scott 2009). Ninety-eigth rudist taxa are present in 48 of these sections and their occurrences can be verified (Table 1, Appendix 2). However it is clear that many more sections with rudists are needed not only to increase rudist diversity but also to extend their ranges to their approximate maximums.

Illustration of Graphic Correlation Method with Rudists

Graphic correlation plots of two sections illustrate the process of interpolating rudist ranges to numerical ages (Figure 2). These two sections control the ages of nineteen species. The X/Y plot shows the FOs as squares and the LOs as plus signs. The inclined line of correlation (LOC) is located by the bioevents considered to be at their maximum ranges in the section on the Y-axis compared to their ages in sections composing the database. Both sections are composed of shallow-water carbonates in which rudists co-occur with age-diagnostic benthic foraminifers; ammonites are also present in the lower part of the Portugal section.

In the Portugal section (Figure 2A) the LOC is constrained by the base of *Neolobites vibrayeanus* (Middle–Upper Cenomanian, Kennedy & Juignet 1984) and the top of *Chrysalidina gradata* (Middle– Upper Cenomanian, Schroeder & Neumann 1985). This LOC position conserves the ranges of most bioevents but does increase the age of one FO and makes younger the LOs of three taxa. Clearly this LOC is one of several hypotheses of correlation, each one of which would project the ages of the rudists within the Middle–Late Cenomanian.

In the Spain section (Figure 2B) the LOC is constrained by the LOs of large benthic foraminifers, *Choffatella decipiens*, *Neotrocholina aptiensis*, and *Palorbitolina lenticularis* and the LOs of *Orbitolina texana* and *Simplorbitolina manasi*. The interpretation of the age projection could be modified slightly by moving the upper part of the LOC to the base of *Simplorbitolina conulus*, which would alter the age of the rudists very slightly. These plots demonstrate how age projections are hypotheses and with graphic correlation technique the ages can be tested and evaluated in a scientific manner.

The bases of the Cretaceous stages are defined in the MIDK4 and MIDK45 databases by the FOs of taxa used in standard time scales including the GSSP for the base of the Cenomanian. The mega-annum scale is based on graphic correlation of key reference sections that contain these taxa, however the scale of MIDK3, the first database, was calibrated to the Harland *et al.* (1990) scale rather than the Gradstein *et al.* (2004) scale. The scale of the MIDK42 database was re-calibrated to accommodate the revised age of the Cenomanian/Turonian boundary, and the ages of other boundaries are very close to the ages of Gradstein *et al.* (2004) except for the age of the base Cenomanian. Although the base Cenomanian has been calibrated to 99.6 Ma (Gradstein *et al.* 2004), new dinoflagellate data support the correlation of the base Cenomanian with the Clay Spur bentonite bed in Wyoming (Oboh-Ikuenobe *et al.* 2007, 2008) dated at 97.17±0.69 Ma (Obradovich 1993). The base of the Barremian is at FO *Assipetra terebrodentarius* at 132.11 Ma (Bralower *et al.* 1995); base Aptian is at FO *Deshayesites oglanensis* at 124.43 Ma; base Albian is at FO *Lemeryella tardefurcata* at 112.66 Ma; base Cenomanian is at FO *Rotalipora globotruncanoides* at 97.13 Ma; base Turonian is at FO *Watinoceras devonense* at 92.95 Ma, which is within the error bar of the 93.5±0.8 Ma age (Gradstein *et al.* 2004).

The X/Y plot compares the rate of sediment accumulation (RSA) in one section with that in the other (Miller 1977). Graphic correlation does not measure the sedimentation rate because the RSA does not account for compaction or other processes that reduce the thickness of the interval from its initial depositional thickness. The technique of graphic correlation enables the stratigrapher to consider sedimentologic events together with the biotic events and test conclusions based on sedimentology with those based on fossils. The interpretation of the two sample sections results in RSA values of 31.85 m/myr and 45.65 m/myr.

Results

The FO and/or the LO of 98 rudist species have been calibrated by one of three methods (Table 1). Graphic correlation analyses of 31 sections, in which rudist species have been reported, produced
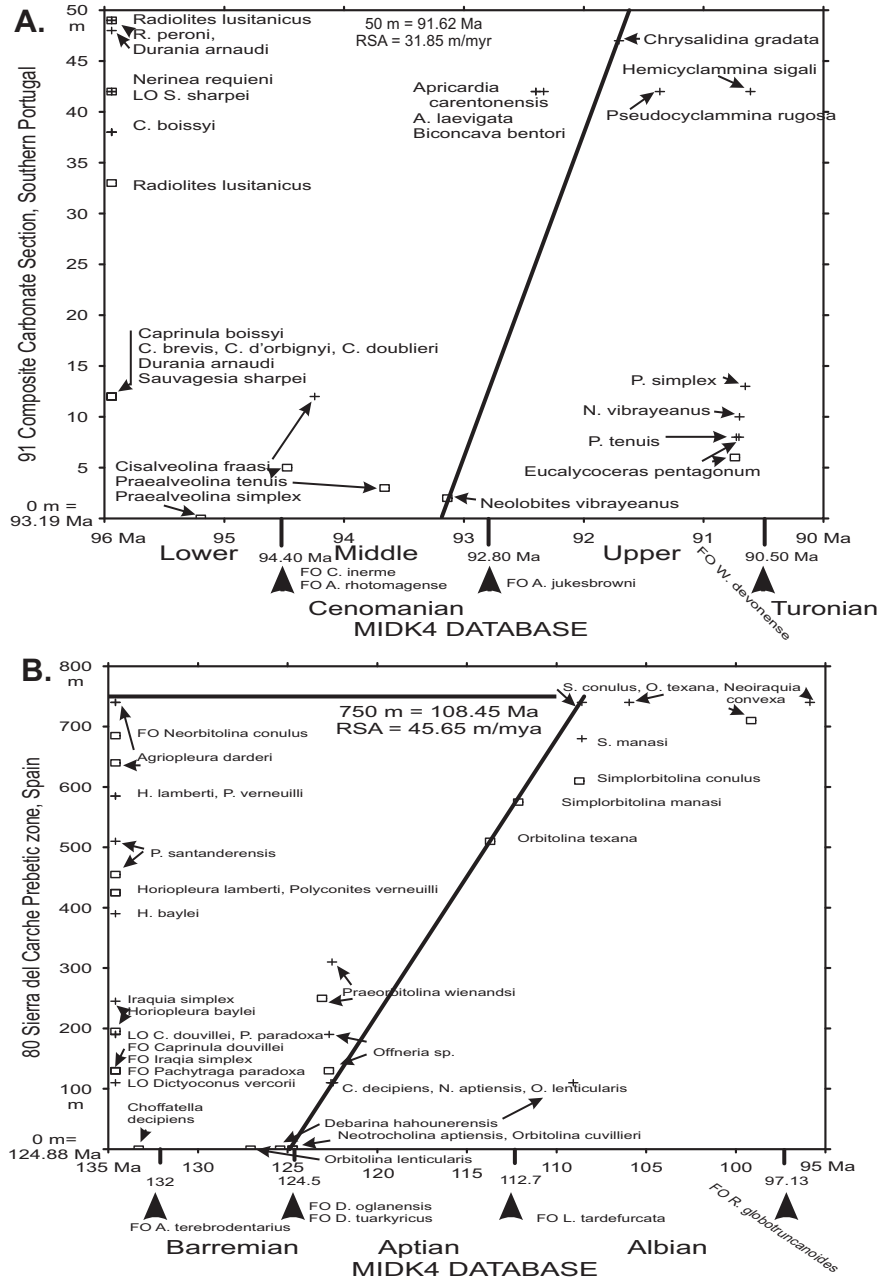
Figure 2. Graphic correlation of two sections that control the ranges of numerous rudist species showing how rudist ranges are calibrated to numerical ages. On Y-axis of each graph the column of squares – FOs and plus-signs – LOs are species occurrences not found in other sections; their numerical ages are interpolated by projecting their metric positions to the line of correlation and down to the Ma time scale on the X-axis. (**A**) Plot of section data from the Leira & Lisbon, Portugal areas composited to the thickness of the Runa section; these strata are called the Cenomanian–Turonian 'Rudist Facies'; the Cretaceous limestone at 50 m is unconformably overlain by Tertiary lava (Berthou 1984, figure 8). This section adds eleven rudist taxa to the MIDK4 database. Note that the age of the Cenomanian/Turonian boundary is not re-calibrated. (**B**) Plot of the section in Sierra del Carche Prebetic zone, Murica, Spain (Masse *et al.* 1992). Base of this section is base of the Bedoulian Substage at base of limestone above sandstone; base Gargasian Substage is at 310 m; base Albian is at 595 m. This section adds eight rudist taxa to the MIDK4 database.
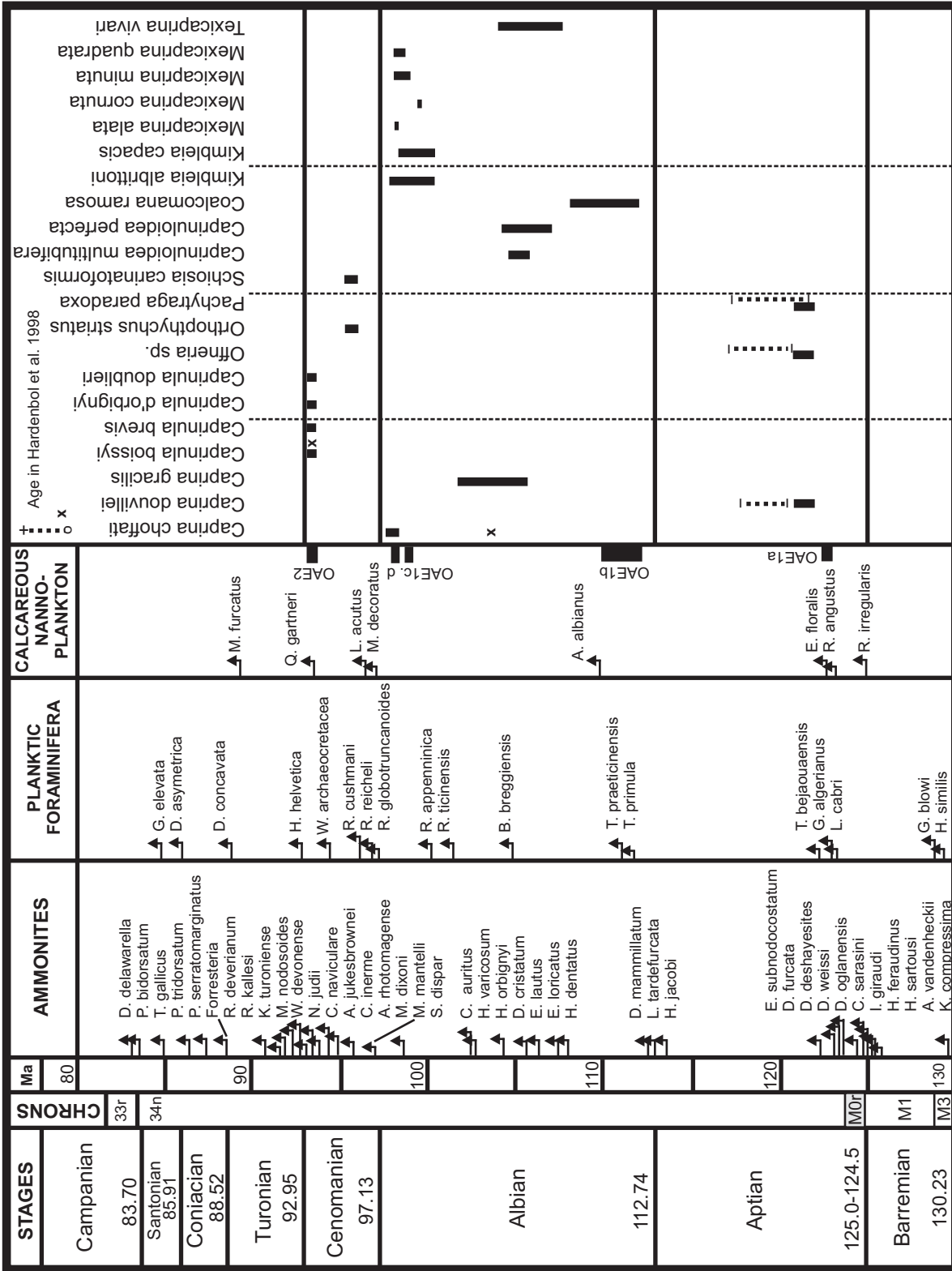
Figure 3. Preliminary stratigraphic ranges of some Caprinuloidea ages calibrated by graphic correlation with ammonites, planktic Foraminifera and calcareous nannoplankton and compared to ages by zonal integration.
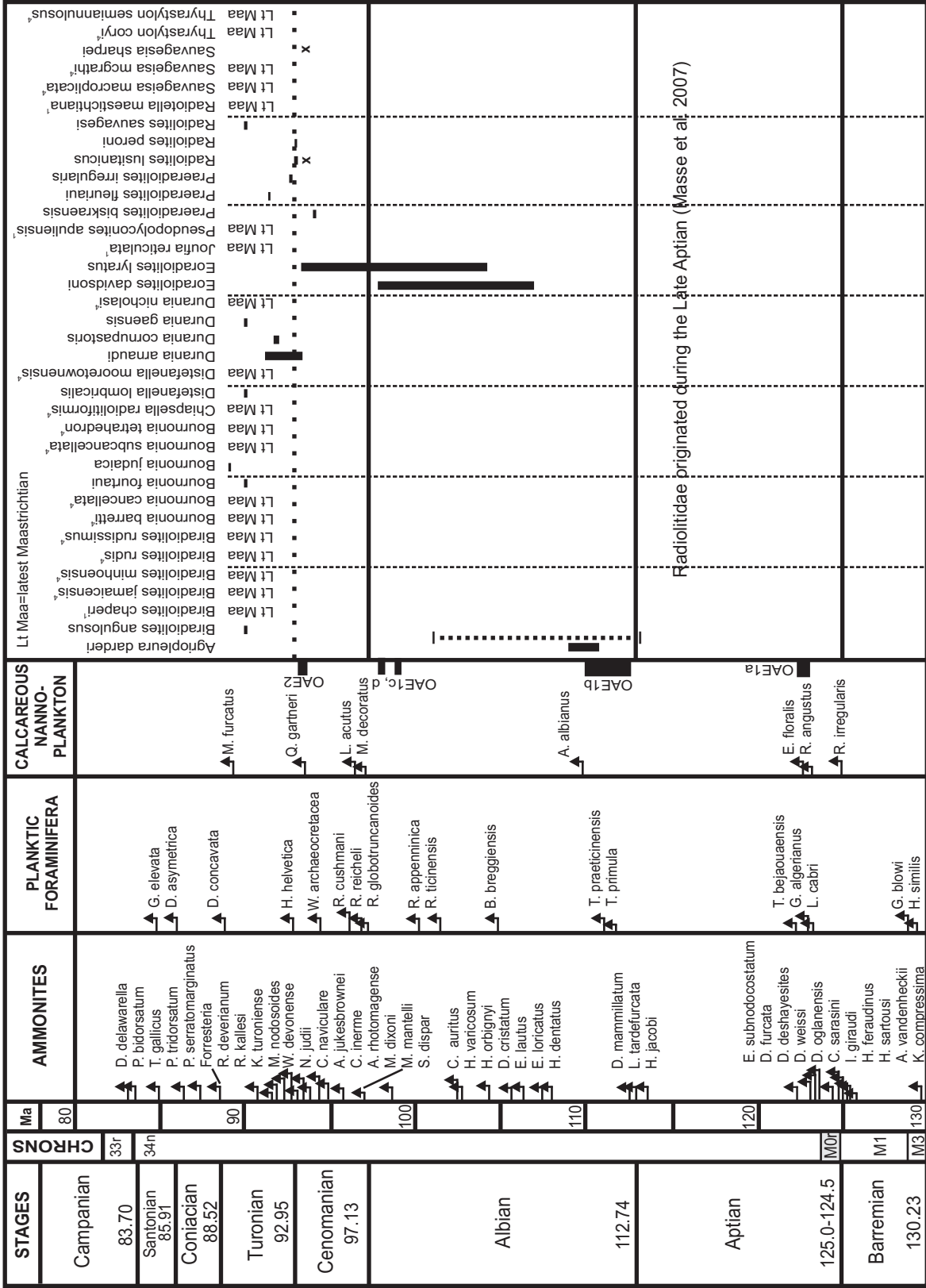
Figure 4. Preliminary stratigraphic ranges of some Radiolitidae ages calibrated by graphic correlation with ammonites, planktic Foraminifera and calcareous nannoplankton and compared to ages by Sr isotopes and zonal integration. Superscripts on some species indicate references of Sr isotope data (see footnote on Table 1).

preliminary numerical ages of the ranges of 57 rudists. This complements ages of 42 taxa derived by Sr isotope analyses (Steuber 2001, 2003; Steuber *et al.* 2002; Steuber & Rauch 2005), and tests the integration of many species with the geologic time scale by correlation with zones and sequence stratigraphy (Hardenbol *et al.* 1998, chart 5). What is clear from the review is that the full ranges of rudist species are incompletely represented so that accurate numerical ages by each method are very preliminary. More detailed measured sections are needed where rudists are associated with age-diagnostic taxa.

Examination of Table 1 shows that of the fifteen taxa dated by both graphic correlation and stage interpolation, six FOs are within a range of less than one million years and seven are older. The LOs of five species are older by graphic correlation than by stage interpolation. This is likely to be the result of too few sections in the database. No species as yet have numerical ages estimated by both graphic correlation and Sr isotope analyses.

Caprinuloidea evolved during the Barremian, diversified during the Albian–Cenomanian, and nearly went extinct during the Cenomanian–Turonian OAE2. This pattern is suggested by the range chart of twenty-one species that are included in the MIDK45 database (Figure 3). The ranges of five have also been dated by zonal integration (Hardenbol *et al.* 1998; on Figure 3 indicated by dashed lines or 'x' marks). The ranges of three Aptian taxa are longer according to Masse (in Hardenbol *et al.* 1998) than calibrated by graphic correlation because they are present in only one or two sections in the MIDK45 database. The age of *Caprina choffati* is about 5–6 myr older by zonal integration than by graphic correlation, in which it occurs in a single section. This suggests that it ranges from middle to latest Albian.

Radiolitidae first appeared in the Late Aptian and diversified after the Cenomanian–Turonian OAE2

(Masse *et al.* 2007). This pattern is suggested by ranges of thirty-five species (Figure 4). The majority of species have been dated by projection of Sr isotope ratios to the Late Cretaceous time scale; two were dated by zone interpolation and sixteen by graphic correlation. The range of *Agriopleura darderi* is dated at about 112 to 100 Ma by Masse (in Hardenbol *et al.* 1998); the age by graphic correlation is 110.86–108.67 Ma based on its occurrence in a single section in Spain, so more sections will extend its range. The ranges of the two species of *Eoradiolites* are very similar to their known ranges and these species are recorded in five and seven sections each. The more sections in which a species is found, the more accurate is the range data.

Conclusions

The accurate calibration of the ranges of rudists to the mega-annum scale will create the potential for their use in precise chronostratigraphy of Cretaceous carbonate carbonate deposits. Normally rudists are diverse and abundant where the traditional biostratigraphic fossils are rare or absent. Consequently standard zonal schemes generally cannot be applied with confidence nor can stage boundaries be correlated into carbonate sections. However the graphic corrrelation method produces a database of carefully documented sections in which rudist ranges can be compared with ranges of biostratigraphically key species.

Acknowledgements

References

Berggren, W.A., Kent, D.V., Aubry, M.-P. & Hardenbol, J. (eds). 1995. *Geochronology, Time Scales and Global Stratigraphic Correlation*. SEPM (Society for Sedimentary Geology) Special Publication **54**.

Berthou, P.-Y. 1984. Albian–Turonian stage boundaries and subdivisions in the western Portuguese Basin, with special emphasis on the Cenomanian–Turonian boundary in the ammonite facies and rudist facies. *Geological Survey of Denmark, Bulletin* **33**, 41–55.

BRALOWER, T.J., FULLAGAR, P.D., PAULL, C.K., DWYER, G.S. & LECKIE, R.M. 1997. Mid-Cretaceous strontium-isotope stratigraphy of deep-sea sections. *Geological Society of America Bulletin* **109**, 1421–1442.

BRALOWER, T.J., LECKIE, R.M., SLITER, W.V. & THIERSTEIN, H.R. 1995. An integrated Cretaceous microfossil biostratigraphy. *In*: BERGGREN, W.A., KENT, D.V., AUBRY, M.-P. & HARDENBOL, J. (eds), *Geochronology, Time Scales and Global Stratigraphic Correlation*. SEPM (Society for Sedimentary Geology) Special Publication **54**, 65–79.

CARNEY, J.L. & PIERCE, R.W. 1995. Graphic correlation and composite standard databases as tools for the exploration biostratigrapher. *In*: MANN, K.O. & LANE, H.R. (eds), *Graphic Correlation*. SEPM (Society for Sedimentary Geology) Special Publication **53**, 23–43.

GRADSTEIN, F., COOPER, R.A. & SADLER, P.M. 2004. Biostratigraphy: time scale from graphic and quantitative methods. *In*: GRADSTEIN, F., OGG, J. & SMITH, A. (eds), *A Geologic Time Scale 2004*. Cambridge University Press, United Kingdom, 49–54.

HARDENBOL, J., THIERRY, J., FARLEY, M.B., JACQUIN, T., GRACIANSKY, P.-C. DE & VAIL, P. 1998. Mesozoic and Cenozoic sequence chronostratigraphyic framework of European basins. *In*: GRACIANSKY, P.-C. DE, HARDENBOL, J., JACQUIN, T. & VAIL, P. (eds), *Mesozoic and Cenozoic Sequence Stratigraphy of European Basins*. SEPM (Society for Sedimentary Geology) Special Publication **60**, 3–13.

HARLAND, W.B., ARMSTRONG, R.L., COX, A.V., CRAIG, L.E., SMITH, A.G. & SMITH, D.G. 1990. *A Geologic Time Scale 1989*. Cambridge University Press, Cambridge.

KENNEDY, W.J. & JUIGNET, P. 1984. A revision of the ammonite faunas of the type Cenomanian. 2. The families Binneyitidae, Desmoceratidae, Engonoceratidae, Placenticeratidae, Hoplitidae, Schloenbachiidae, Lyelliceratidae and Forbesiceratidae. *Cretaceous Research* **5**, 93–161.

MASSE, J.-P., ARIAS, C. & VILAS, L. 1992. Stratigraphy and biozonation of a reference Aptian–Albian p.p. Tethyan carbonate platform succession: the Sierra del Carche series (oriental Prebetic zone – Murica, Spain). *Austrian Academy of Science* **9**, 201–221.

MASSE. J.-P., FENERCİ-MASSE, M., VILAS, L. & ARIAS, C. 2007. Late Aptian–Albian primitive Radiolitidae (bivalves, hippuritoidea) from Spain and SW France. *Cretaceous Research* **28**, 697–718.

MCARTHUR, J.M. & HOWARTH, R.J. 2004. Strontium isotope stratigraphy. *In*: GRADSTEIN, F., OGG, J. & SMITH, A. (eds), *A Geologic Time Scale 2004*. Cambridge, U.K., Cambridge University Press, 96–105.

MCARTHUR, J.M., HOWARTH, R.J. & BAILEY, T.R. 2001. Strontium isotope stratigraphy: Lowess Version 3: Best-fit to the marine Sr-isotope curve for 0 to 509 Ma and accompanying look-up table for deriving numerical age. *Journal of Geology* **109**, 155–170.

MILLER, F.X. 1977. The graphic correlation method in biostratigraphy. *In:* KAUFFMAN, E.G. & HAZEL, J.E. (eds), *Concepts and Methods of Biostratigraphy*. Dowden, Hutchinson & Ross, Inc., Stroudsburg, Pa., 165–186.

OBOH-IKUENOBE, F.E., BENSON, D.G., JR., SCOTT, R.W., HOLBROOK, J.M., EVETTS, M.J. & ERBACHER, J. 2007. Re-evaluation of the Albian–Cenomanian Boundary in the U.S. Western Interior based on Dinoflagellate Cysts. *Review of Palaeobotany and Palynology* **144**, 77–97.

OBOH-IKUENOBE, F.E., HOLBROOK, J.H., SCOTT, R.W., AKINS, S.L., EVETTS, M.J., BENSON, D.G., JR. & PRATT, L.M. 2008. Anatomy of epicontinental flooding: Late Albian–Early Cenomanian of the Southern U.S. Western Interior basin. *In*: PRATT, B.R. & HOLMDEN, C. (eds), *Dynamics of Epeiric Seas*. Geological Association of Canada, Special Paper **48**, 201–227.

OBRADOVICH, J.D. 1993. A Cretaceous time scale. *In*: CALDWELL, W.G.E. & KAUFFMAN, E.G. (eds), *Evolution of the Western Interior Basin*. Geological Association of Canada Special Paper **39**, 379–396.

ROBASZYNSKI, F., CARON, M., AMÉDRO, F., DUPUIS, C., HARDENBOL, J., GONZALEZ DONOSO, J.M., LINARES, D. & GARTNER, S. 1993. Le Cénomanien de la région de Kalaat Senan (Tunisie centrale): Litho-biostratigraphie et interprétation séquentielle. *Revue de Paléobiologie* **12**, 351–505.

ROBASZYNSKI, F., CARON, M., DUPUIS, C., AMEDRO, F., GONZALEZ DONOSO, J.-M., LINARES, D., HARDENBOL, J., GARTNER, S., CALANDRA, F. & DELOFFRE, R. 1990. A tentative integrated stratigraphy in the Turonian of central Tunisia: formations, zones and sequential stratigraphy in the Kalaat Senan area. *Centres Recherches Exploration Production Elf-Aquitaine, Bulletin* **14**, 213–384.

SARI, B. 2006. Upper Cretaceous planktonic foraminiferal biostratigraphy of the Bey Dağları autochthon in the Korkuteli Area, Western Taurides, Turkey. *Journal of Foraminiferal Research* **36**, 241–261.

SARI, B., STEUBER, T. & ÖZER, S. 2004. First record of Upper Turonian rudists (Mollusca Hippuritoidea) in the Bey Dağları carbonate platform, Western Taurides (Turkey): taxonomy and strontium isotope stratigraphy of *Vaccinites praegiganteus* (Toucas, 1904). *Cretaceous Research* **25**, 235–248.

SCHROEDER, R. & NEUMANN, M. 1985. *Les grand foraminifères du Crétacé moyen de la région Méditerranénne*. Geobios, Mémoire Spécial **7**.

SCOTT, R.W. 2009. Chronostratigraphic database for Upper Cretaceous Oceanic Red Beds (CORBs). *In*: HU, X., WANG, C., SCOTT, R., WAGREICH, M. & JANSA, L. (eds), *Cretaceous Oceanic Redbeds: Stratigraphy, Composition, Origins, and Paleoceanographic and Paleoclimatic Significance*. SEPM (Society for Sedimentary Geology) Special Publication **91**, 35–57.

SCOTT, R.W., SCHLAGER, W., FOUKE, B. & NEDERBRAGT, S.A. 2000. Are Mid-Cretaceous eustatic events recorded in Middle East carbonate platforms?. *In*: ALSHARHAN, A.S. & SCOTT, R.W. (eds), *Middle East Models of Jurassic/Cretaceous Carbonate Systems*. SEPM (Society for Sedimentary Geology) Special Publication **69**, 77–88.

STEUBER, T. 2001. Strontium isotope stratigraphy of Turonian–Campanian Gosau-type rudist formations in the Northern Calcareous and Central Alps (Austria and Germany). *Cretaceous Research* **22**, 429–441.

STEUBER, T. 2002. Plate tectonic control on the evolution of Cretaceous platform-carbonate production. *Geology* **30**, 259–262.

STEUBER, T. 2003. Strontium isotope chemostratigraphy of rudist bivalves and Cretaceous carbonate platforms. *In*: GILI, E., NEGRA, M.H. & SKELTON, P.W. (eds), *North African Cretaceous Carbonate Platform Systems*. NATO Science Series, Earth and Environmental Sciences **28**, 229–238, Kluwer Academic, Dordrecht.

STEUBER, T., MITCHELL, S.F., BUHL, D., GUNTER, G. & KASPER, H.U. 2002. Catastrophic extinction of Caribbean rudist bivalves at the Cretaceous/Tertiary boundary. *Geology* **30**, 999–1002.

STEUBER, T., PARENTE, M., HAGMAIER, M., IMMENHAUSER, A., VAN DER KOOIJ, B. & FRIJIA, G. 2007. Latest Maastrichtian species-rich rudist associations of the Apulian Margin of Salento (S Italy) and the Ionian Islands (Greece). *In*: SCOTT, R.W. (ed), *Cretaceous Rudists and Carbonate Platforms: Environmental Feedback*. SEPM (Society for Sedimentary Geology) Special Publication **87**, 151–157.

STEUBER, T. & RAUCH, M. 2005. Evolution of the Mg/Ca ratio of Cretaceous seawater: implications from the composition of biological low-Mg calcite. *Marine Geology* **217**, 199–213.

STEUBER, T., YILMAZ, C. & LOSER, H. 1998. Growth rates of Early Campanian rudists in a siliciclastic-calcareous setting (Pontide Mts., North-Central Turkey). *Geobios, Mémoire Spécial* **22**, 385–401.

Appendix 1. Rudist-bearing localities of MIDK45 Database: Group numbers are located on Figure 1.

GROUP 1

Section Name: Lampazos, Sonora Section; Mural 1 Lampazos Area Composite Section

Location: Sonora, Mexico

Author: Scott & Gonzalez-Leon 1991, *GSA Special Paper* **254**, 52–67.

Stratigraphy: Sections 2 and 4 are stacked on base of Espinazo Del Diablo Formation at 1090 m in section 2.

Section Name: Mural Composite of Eight Sonoran and Arizonan Sections

Location: Sonora Mexico and Arizona

Author: Scott & Gonzalez-Leon 1991, *GSA Special Paper* 254, 52–67; Gonzalez-Leon *et al.* 2008, *Cretaceous Research* **29**, 249–266.

Stratigraphy: Albian Mural Formation and equivalent units.

Mural 1– Lampazos Area Composite Section; Sections 2 and 4 are stacked on base of Espinazo Del Diablo Formation at 1090 m in section 2.

Mural 2– Santa Ana Section, Sonora; Base Cerro La Ceja= 0 m; base Tuape= 100 m; base Los Coyotes= 310 m; base Cerro La Puerta= 410 m; base Cerro La Espina= 450 m; base Mesa; Quemada= 615 m.

Mural 3– Cerro Pimas Section, Sonora; Base Cerro La Ceja= 0 m; base Tuape= 55 m; base Los Coyotes= 150 m; base Cerro La Puerta= 205 m; base Cerro La Espina= 325 m; base Mesa Quemada= 360 m.

Mural 4– El Ocuca Section, Sonora; Base Cerro La Ceja= 0 m; base Tuape= 50 m; base Los Coyotes= 250 m; base Cerro La Puerta= 330 m; base Cerro La Espina= 435 m; base Mesa Quemada= 475 m.

Mural 5– Grassy Hill Section, Cochise County, Arizona; W1/2, SE, sec. 12, T23S, R24E;
Base of section in Lower Mural; base Upper Mural 29 m; base Cintura Formation 96 m.

Mural 6– Paul Spur Section-East face, Cochise County, Arizona; W1/2 NE NE NE, sec. 1, T24S, R25E; 31.37754N, 109.75285W. Base of section in Lower Mural; base Upper Mural 10m; top of section in Upper Mural= 21m.

Mural 7– Tuape Section, Sonora; Base Cerro La Ceja= 0 m; base Tuape= 185 m; base Los Coyotes= 370 m; base Cerro La Puerta= 500 m; base Cerro La Espina= 600 m; base Mesa Quemada= 625 m.

Mural 8– Rancho Bufalo Section, Sonora; Base Fronteras Member .= 0 m; base Rancho Bufalo Member= 130 m; base Cerro La Ceja= 250 m; base Tuape= 320m; base Los Coyotes= 445 m; base Cerro La Puerta= 535 m; base Cerro La Espina= 590 m, top section= 660 m.

GROUP 2

Section Name: MIDK 18-Shell No. 1 Chapman Core, Texas

Location: Shell No. 1 Chapman Core, Waller Co., Texas

Author: Data in Scott 1990, *SEPM Concepts* **2**, p. 82.

Stratigraphy: Aptian–Upper Albian carbonate platform forereef basin to shelf margin. Contact of Fredericksburg/Washita Group: Marker bed Al SB WA 1 17,140 ft; base Tamaulipas Formation above Pearsall Formation: Marker bed Al SB GR 1 12,025 ft.; base Pearsall Formation on Sligo Formation: Marker bed Ap SB PR 1 20,075 ft. Total depth at 20,800 ft

Section Name: MIDK 19-Shell No. 1 Tomasek Core, Texas

Location: Shell No. 1 Tomasek, Bee Co., Texas

Author: Scott 1990, *SEPM Concepts* **2**, p. 82.

Stratigraphy: Lower–Upper Albian carbonate platform forereef basin to shelf margin. Top of Fredericksburg Group: Marker bed Al SB WA 1 13 420 ft; top of Tamaulipas, Formation 14,550 ft; total depth at 15,407 ft.

Section Name: MIDK 21-Austin, Texas Composite Section

Location: Austin, Texas Composite section, Travis Co. Sections selected along TX 1431.

Author: Data from Young 1974, *Geoscience* & *Man* **8**, 175–228; Perkins, ibid, 131–174. Amsbury 1988, *GSA Centennial Field Guide-S-Central*, 373–376; enhanced by personal observations by R. W. Scott & E. Mancini 2003.

Stratigraphy: Upper Aptian–Lower Cenomanian mixed carbonate & clastics platform. base Pepper Shale above Buda Formation. 1302 ft; base Del Rio Formation Grayson Formation. 1265 ft; base Washita Gp. on Edwards Formation (top Fredericksburg Gp.) 1196 ft; base Walnut Formation 836 ft; 6m below base 'Corbula marker bed' in mid Glen Rose Formation 460 ft.; base lower Glen Rose Member 200 ft; base Hensel Formation above Cow Creek Formation= James Ls. downdip 160 ft; base Sycamore Sandstone above Paleozoic rocks= base Pearsall Formation. 0 ft.

Section Name: MIDK 21B Colorado River Composited Section

Location: Sections selected along TX 1431 with additional data from Hamilton State Park;

Author: Amsbury 1988, *GSA Centennial Field Guide, South Central Geological Society*, 373–376; Lozo & Stricklin 1956, *GCAGS* **6**, 67–78, figures 5, 6, 7; Martin 1967, *Permian Basin SEPM* 67–8, 286–299, figure 2, #6; Moore 1964, *BEG Rpt. Invest.* 52, figure 6; Stricklin *et al.* 1971, *BEG Rpt. Invest.* 71, figures 9, 10; Wilbert 1967, *Permian Basin SEPM* 67–8, 256–285, plate 1, # 13, 14; Young 1974, *Geoscience* & *Man* **8**, 175–228; Perkins, ibid, 131–174; Young 1977, *Guidebook to the geology of Travis County*, U. Texas department publication; enhanced by personal observations by R. W. Scott.

Stratigraphy: Upper Aptian–Lower Cenomanian mixed carbonate & clastics platform as in MIDK20.

Section Name: MIDK 85 Blanco River, TX Composited Section

Location: Blanco-Guadalupe River Composite Section, Kendall, Comal, Hays counties, Texas.

Author: see below

Stratigraphy: Upper Aptian–Lower Cenomanian mixed carbonate & clastics platform.

Section Segments: Buda Ls. 50 ft thick, top at 381 m, unconf. at 30 ft, sections 1, 2 (Martin 1967, *Permian Basin SEPM* 67–8, p. 289, figure 2, #6); Intra-Buda unconformity at 375 m; Buda ammonites (Young 1979, p. 83–84); Del Rio Shale 60 ft thick, top at 366 m; Wilbert 1967, *Permian Basin SEPM* 67–8, 256–285, plate 1, #13, 14; Georgetown Formation 45 ft thick, top at 347.6 m (Barnes 1974, Seguin Sheet, Tx Atlas); Edwards Ls. 275 ft thick, top at 334 m, Bee Cave Marl 5' thick, top at 250 m (Moore 1964, *BEG*

Appendix 1. Continued.

Rpt. Invest. 52, figure 6); Bull Creek Ls. Member. 40 ft thick, top at 248 m; Upper Glen Rose Member 400 ft thick at Seven H Ranch, top at 236 m; Lower Glen Rose Member 255 ft thick at Blanco Creek, top at 114 m (Stricklin *et al.* 1971, *BEG Rpt. Invest.* 71, figures 9, 10; Lozo & Stricklin 1956, *GCAGS* **6**, 67–78, figures 5, 6, 7; Narrows biostrome at 50–60 m; Pipe Creek biostrome at 77–93 m; Hensel Formation 45 ft thick at Edge Ranch, top at 36.6 m (Amsbury et al., 1999 unpublished); Cow Creek Ls. 35 ft thick, Edge Ranch, top at 23 m (Amsbury *et al.* 1999, unpublished); Hammett Shale not fully exposed, top at 12 m; Ammonites in Young 1974, *Geoscience* & *Man* **8**, 175–228; Perkins, ibid, 131–174; enhanced by personal observations by R.W. Scott (2003; Scott *et al.* 2007, *SEPM SP* **87**, 181–191).

Section Name: MIDK 89 Stanolind #1 Schmidt, Guadalupe Co.
Location: Stanolind No. 1 Schmidt, Guadalupe Co., Texas, cored 1072-1910 ft and 2200-2610 ft.
Author: Microfossil thin section Data by Scott, 1982, unpublished data. Palynomorph data by R.W. Hedlund, 1982, unpubl.
Stratigraphy: Aptian–Upper Albian carbonate platform to shelf margin. Base Woodbine Ss. over Buda Ls. at -280 ft; base Del Rio Shale at -340 ft; top Fredericksburg Group/base Washita Group at -490; base Glen Rose Formation above Pearsall Formation at -1802 ft; base Pearsall Formation on Sligo Formation at -1980 ft; TD at 2640 ft.

Section Name: MIDK 117 Pioneer No. 1 Schroeder, Bee Co.
Location: Pioneer No. 1 Schroeder, Bee County, Texas
Author: Lowell Waite *et al.* 2007, *GCAGS Proceedings*; paleo data by R.W. Scott.
Stratigraphy: Top core at 13798 ft; Top Stuart City Formation at 13798 ft; base core 14749 ft.

Section Name: MIDK 96 4898 # 2, Chandeleur Sound, Louisiana
Location: State Lease 4898 #2, Chandeleur Sound, Louisiana
Author: New core samples 15 July 2004, E.A. Mancini & R.W. Scott. Unpubl. thin section analyses by R.W. Scott 1980; *Palynology* by D.G. Benson, 08/2004.
Stratigraphy: Aptian–Albian cabonate shelf facies. Tied to seismic by M. Badali, U. Alabama, Ph.D. Four core segments (12810-12851.5 ft, 13543-13565 ft, 13624-13708 ft, & 14199-14245 ft) examined July 2004 by E.A. Mancini, R.W. Scott & J.C. Llinas.

Section Name: Pecos River Comp. Std. Section, TX
Location: Val Verde County, Texas.
Author: Scott & Kidson 1977, *BEG, U. Tx., Rpt. Invest.* **89**, p. 173; Scott 1990, *SEPM Concepts Series* v. **2**, p. 67; Kerans *et al.* 1999, *SEPM Guideboook*.
Stratigraphy: Albian units in West Texas.
Pecos. 1 – Ft. Stockton Composite section. East Mesa section exposes Antlers Formation 0–50 ft; Ft. Terrett Formation 50–215 ft; Segovia Formation 215–516 ft; Burt Ranch Member . 215–290 ft; 'Boracho Formation' 155–335 ft; Big Mesa quarry exposes Boracho and 'Ft. Lancaster Formation' with base at 335 ft. Sample 1 at Big Mesa section= 334 ft at East Mesa section; base mid cap rock= 396 ft; base upper cap rock= 492 ft, top of section= 516 ft.

Pecos. 2 – Hwy 90 Section RWS.2; Top Buda= 408.1 ft; top Del Rio= 357.1 ft; top Devils River= 339.7 ft; top Salmon Peak= 222 ft; top McKnight= -45 ft; top West Nueces Formation= -130 ft.; composited lower section from core ID-1 in Kerans 1999 correlation chart.
Pecos. 3 – Hwy 90 Section CK.3; Kerans section in 1999 SEPM Guidebook, p. 93.
Pecos. 4 – Ladder Section.4; Kerans section in 1999 SEPM Guidebook.
Pecos. 5 – Harkell Section.5; Kerans section in 1999 SEPM Guidebook.
Pecos. 6 – Painted Canyon Section 6, Pecos River, Val Verde Co., Tx; section in 1999 SEPM Guidebook, p.16, figure 7.
Pecos. 7 – Lewis Canyon Section.7, section C in SEPM 1999 Guidebook, p. 81, Fig. L8.
Pecos. 8 – 2_16_1 Section.8; Kerans section in 1999 SEPM Guidebook, p. 85.
Pecos. 9 – Deadman Canyon Section.9; Kerans section in 1999 SEPM Guidebook, p. 89.
Pecos. 10 – Hoodoo Canyon Section; List of sequence boundaries from Kerans in 1999 SEPM Guidebook, Pl. 1.
Pecos. 11 – WFLZ RR Bridge Section.1; Kerans section in 1999 SEPM Guidebook, p. PC90-8.

Section Name: UPK.1 Austin Group Composite Section
Location: Austin Texas area.
Author: Young & Woodruff 1985, *Austin Geological Society Guidebook* **7**.
Stratigraphy: Section data in figures 1, 2; p. 25, 43. Base of section at 0 meters is base of Austin Group; negative positions are in South Bosque Fm.

GROUP 3
Section Name: MIDK 91 Composite Carbonate Section
Location: Southern Portugal
Author: Berthou 1984, *Bulletin of Geological Survey of Denmark* **33**, 41–55, figure 8.
Stratigraphy: Composited data from Leira & Lisbon areas plotted to thickness of the Runa section; considered to be the Cenomanian 'Rudist Facies'; top at 50 m is unconformity with Tertiary lava.

Section Name: MIDK 92 Composite Section
Location: Composite Section, Portugal
Author: Berthou 1984, *Bulletin of Geological Survey of Denmark* **33**, 41–55, figure 2.
Stratigraphy: Aptian/Albian section; major unconformity at 15 m between carbonate below and conglomerate above.

GROUP 4
Section Name: MIDK 80 Sierra del Carche Prebetic zone, Spain
Location: Prebetic zone, Murica, Spain
Author: Masse *et al.* 1992, Band 9, *Austrian Academy of Science*, 201–221.
Stratigraphy: Base section is base Bedoulian, base Gargasian at 310 m; base Albian at 595 m; base of section is at base of limestone above sandstone.

GROUP 5
Section Name: MIDK 101 Font-Blance, France Cenomanian–Turon
Location: Font-Blance, France
Author: J. Philip 1998, *SEPM SP* **60**, 387–395; data from figure 3, p. 390.

Appendix 1. Continued.

Stratigraphy: Cenomanian–Turonian reference section for sequence stratigraphy on a platform in SE France.

GROUP 6
Section Name: MIDK 22-Nahr Ibrahim, Lebanon, Alb-Cen
Location: Nahr Ibrahim Section, Lebanon
Author: Saint-Marc, 1974, Notes et Mem. sur le Moyen-Orient, v. 13, Mus. Nat. d'Histoire Naturelle, p. 37–43, figure 8. Ammonite data from Saint-Marc 1981 in Reyment & Bengston, Aspects of Mid-Cretaceous Regional Geology, Academic Press, p. 103–131
Stratigraphy: Albian–Cenomanian carbonate platform. Sectioin divided into informal facies intervals; taxa assumed to range throughout the units.

GROUP 7
Section Name: MIDK 16-Wadi Miaidin, Oman, Scott, 1990, Alb–Cenomanian
Location: Wadi Miaidin Outcrop section, Jebel Akhdar, Oman.
Author: Scott 1990, *Geological Society, London, Special Publications* **49**, p. 94–96.
Stratigraphy: Section extends from Aptian/Albian to uppermost Cenomanian. Top Wasia Group 4836 ft top Cenomanian at unconformity; Top B Member 4750 ft; Top C Member 4600 ft; Top D Member 4370 ft; Top E Member 4310 ft; Top F Member 3930 ft; Top G Member 3890 ft; Top Nahr Umr Formation 3835 ft, base 3240 ft in unconformable contact with Shuaiba Formation; Top Albian 3800 ft based on graphic correlation in Scott 1990; Top Lower Cenomanian 4245 ft; Top Middle Cenomanian 4685 ft.

Section Name: MIDK 16B Wadi Miaidin, Oman, Scott, 1990, Berriasian–Aptian
Location: Same section as MIDK16 with Thamama Group data added 06/02.
Author: Scott 1990, *Geological Society, London, Special Publications* **49**, p. 94–96.
Stratigraphy: Top Jurassic 571 ft; top Rayda 700 ft; top Salil 1800 ft; top Habshan 2120 ft; Top Lekhwair 2550 ft; top Kharaib 2975 ft; top Shuaiba 3240 ft (Scott, fig. 6); Top Nahr Umr Formation 3835 ft, base 3240 ft in unconformable contact with Shuaiba Formation; Top Wasia Group 4836 ft at top Cenomanian at unconformity.

Section Name: MIDK 47-Wadi Mi'aidin, Oman
Location: Wadi Mi'aidin, Oman
Author: Philip *et al.* 1995, *Paleo-3* **119**, 77–92. Taxa recorded in figure 3, p. 79; species assignments based on reports by Simmons & Hart (1988) and Scott (1990).
Stratigraphy: Base of section at 0 m= base Natih Formation, top Natih at 280 m with Muti Formation Sequence boundaries of van Buchem *et al.* (1996, 1997): SB at 0, 48, 78, 127, 136, 166, 178, 215?, 280 m.

Section Name: MIDK 75 North Huqf, Oman, section S 001
Location:
Author: Immenhauser *et al.*, unpublished, June 2002
Stratigraphy: Large-scale sequences at 3.1 m, 36.9 m, 61.5 m at top of section; medium-scale sequences at 3.1 m, 8.2 m, 21.4 m, 30.5 m, 36.9 m, 43.8 m,55.5 m.

Section Name: MIDK 76 North Huqf, Oman, section S 008
Location:
Author: *Immenhauser *et al.*, unpublished June, 2002
Stratigraphy: Shuaiba Formation, partial cycle 0–12.5 m.

Section Name: 400 Wadi Bani Kharus, Oman
Location: Wadi Bani Kharus, Oman
Author: A. Immenhauser
Stratigraphy: Section measured 6-11-96; measurements begin at 0 m at Shuaiba/Nahr Umr contact so 10 m added; Top Nahr Umr Formation at 117.2 m

Section Name: 406 Wadi El Assyi, Oman
Location: Oman
Author: A. Immenhauser
Stratigraphy: Al Hassanat Formation, Oman; section measured 14-01-99 measurements begin at 0 m in Al Hassanat Formation; so 10 m added; add 26 m to all fossil positions (04-2000); top of section at 183 m.

GROUP 8:
Section Name: MIDK.1 Kalaat Senan outcrop section.
Location: El Kef, Tunisia.
Author: Robaszynski *et al.* 1990, *BCREP Elf* **14**, 213–384.
Stratigraphy: Upper Cen-Coniacian. Section assumed to record continuous & uniform sediment accumulation at 0.04 cm/ka. Reference section for Turonian cycles interpreted by Hardenbol.

Section Name: MIDK.10 Kalaat Senan.
Location: Tunisia.
Author: Robaszynski *et al.* 1994, *Revue du Paleobiologie* **12**, 351–505.
Stratigraphy: Composited Cenomanian outcrop sections tied by means of lithologic marker beds. Cen/Tur boundary between 742–745 m based on ammonites and 738 m at base of *Q. gartneri*. Taxonomic editing by S. Nederbragt, 4 Ap 95. Alb/Cen boundary at 94 m by base of *R. globotruncanoides* w/ top *Mortoniceras* sp. Reference section for Cenomanian cycles interpreted by Hardenbol 14/7/96. Top Fahdene Formation at 722m. Top Bahloul Formation at 745m. Top of section at 1032m in Annaba Formation. SB @ 78, 207, 318, 406.5, 623, 717.5

GROUP 9
Section Name: MIDK 66 Jebel Areif El Naqa, Sinai, Egypt
Location: Section AN, N30º 21'23", E34 º 26'00";
Author: Bauer, Marzouk, Steuber & Kuss 2001, *Cretaceous Research* **22**, 497–546; Bauer *et al.* 2004, *Cour. Forsch. Senck* **247**, 207–231;
Stratigraphy: Use thicknesses in figure 6 (2004); base section at 0 m in Halal/Raha Formation, base lower Abu Qada Formation at 45 m; base middle at 74 m, base upper at 86 m, base Wata Formation at 103 m, top section at 155 m. Sampled interval N5 49-94 m (p. 516, 2001) (= 45–102 m in figure 6, 2004). Cenomanian/Turonian unconformity at base Abu Qada Formation Sequence stratigraphy from Bauer *et al.* (2004): CeSin 7 at 45 m; TuSin 1 at 84 m;

Appendix 1. Continued.

Section Name: MIDK 67 Gebel Abu Zurub, Sinai, Egypt
Location: Section Z, N29 º 22'31", E33 º 21'07";
Author: Bauer, Marzouk, Steuber, & Kuss 2001, *Cretaceous Research* **22**, 497–546; Bauer *et al.* 2004, *Courier Forschung. Senckenberg* **247**, 207–231, figure 8; Use thicknesses on figure 8 (2004).
Stratigraphy: Base section at 0 m in Raha Formation; base lower Abu Qada Formation at 82/75 m, base middle at 100/93 m, base upper at 122/115 m; base Wata Formation at 181 m; top section at 200/158 m. Sampled intervals N2 12-62 m (p. 515) (= 19–70 m figure 8, 2004); N9 77-90 m (= 82–95 m on figure 8, 2004), N8 136-144 m (p. 516) (= 142–150 m on figure 8, 2004). Cenomanian/Turonian unconformity at base Abu Qada at 82 m (75 m in figure 4, 2001); Section measurements in figure 8 (2004); Sequence stratigraphy: Bauer *et al.* (2004): CeSin6 at 9 m; CeSin7 at 75 m; TuSin1 at 122 m.

Section Name: MIDK 68 Gebel Guna, Sinai, Egypt
Location: Section G, N28 º 56'09", E34 º 05'48".
Author: Bauer, Marzouk, Steuber & Kuss 2001, *Cretaceous Research* **22**, 497–546.
Stratigraphy: Base section at 0 m in Raha Formation, base Abu Qada Formation lower at 66 m, base middle at 85 m; base upper at 92 m, base Wata Formation covered at 117 m, top section at 137 m. Sampled intervals N3 28-49 m, N10 67-78 m (p. 515-516). Cenomanian/Turonian unconformity at base Abu Qada Formation. Section Q stacked above at Wata/Matulla contact at 187 m assuming Wata is 70 m thick; so top of composited section is 226 m; data from figure 13, p. 517.

Section Name: MIDK 109 Gabal El Minsherah, North Sinai
Location: Gabal El Minsherah, North Sinai.
Author: Felieh 2007, manuscript, figures 2, 4.

Stratigraphy: Halal Formation 0–218 m; Wata Formation 218–290 m; contact is Cenomanian/Turonian boundary. Estimated positions of sequence boundaries of Bauer *et al.* 2004, *Courier Forschungen* **287**: CeSin 6-122 m; CeSin 7-206 m; TuSin 1-246.5 m; TuSin 2-274 m.

Section Name: MIDK 110 Gabal Yelleg,
Location: North Sinai
Author: Felieh 2007, manuscript, figures 2, 4
Stratigraphy: Halal Formation 0–450 m; Wata Formation 450–575 m; boundary is C/T. Hardgrounds at 306 m, 415m, 520 m.

GROUP 10
Section Name: UPK 38 Section 1, Bey Dağları, Turkey
Location: Section 1, Bey Dağları, Turkey, on Rt. E87 a few km SW of Korkuteli.
Author: Sarı 2006, *Journal of Foraminiferal Research* **36**, 241–261, figure 4.
Stratigraphy: Top Bey Dağları Formation 0–18.8 m at regional hardground, top Akdağ Formation 27 m unconformity below Paleogene; *D. concavata* Interval Zone 4–9.5m; top *D. asymetrica* Total Range Zone 18.7 m; top *G. gansseri* I.Z. 27 m.

GROUP 11
Section Name: MIDK 73 Cres Island, Croatia section
Location: Cres Island, Croatia section, approx. 45 º N, 14 º 30' E
Author: Section composited from sections measured by Dragozetici, Petrovski & Baldarin in Husinec *et al.* 2000, *Cretaceous Research* **21**, 155–171.
Stratigraphy: Composite section in figure 2; segment 1: 46–86 m in figure 3a; segment 2: 138–188 m in figure 3b; segment 3: 321–368 m in figure 3c; segment 4: 593–618 m in figure 9A; segment 5: 843–880 m in figure 9B. Estimated stage bases: Aptian at 46 m; Albian at 125 m; Cenomanian at 500 m. Successive emersion beds from 110–140 m may correspond to intra-Aptian emergence event (p. 157).

Appendix 2. Rudist taxa in MIDK45 Database. Maximum age values of taxa for sections in MIDK 3, 4, 41, 42, 45 databases (as of 08/12/2008). Number in front of section name is computer file number.

Agriopleura darderi		
80 Sierra del Carche Prebetic zone, Spain	110.86	108.67
	110.86	108.67
Apricardia carentonensis		
91 Composite Carbonate Section, Portugal	93.17	93.13
92 Composite Section, Portugal	95.98	93.24
	95.98	93.13
Apricardia laevigata		
101 Font Blanc, France	93.22	93.14
91 Composite Carbonate Section, Portugal	93.17	93.13
92 Composite Section, Portugal	95.98	93.24
	95.98	93.13
Biradiolites angulosus		
66 Jebel Areif El Naqa, Sinai, Egypt	90.32	89.99
	90.32	89.99
Bournonia fourtaui		
66 Jebel Areif El Naqa, Sinai, Egypt	90.32	89.99
	90.32	89.99
Bournonia judaica		
66 Jebel Areif El Naqa, Sinai, Egypt	88.95	88.95
	88.95	88.95
Caprina choffati		
92 Composite Section, Portugal	99.19	98.86
	99.19	98.86
Caprina douvillei		
80 Sierra del Carche Prebetic zone, Spain	122.03	120.72
	122.03	120.72
Caprina gracilis		
21-Austin, Texas Composite Section,	104.03	101.81
21B Colorado River Composited Section	105.09	105.06
85 Blanco River, TX Composited Section	105.53	105.49
	105.53	101.81
Caprinula boissyi		
91 Composite Carbonate Section, Portugal	93.45	93.17
	93.45	93.17

Appendix 2. Continued.

Caprinula brevis		
91 Composite Carbonate Section, Portugal	93.45	93.17
	93.45	93.17
Caprinula d'orbignyi		
101 Font Blanc, France	93.44	93.38
91 Composite Carbonate Section, Portugal	93.45	93.17
	93.45	93.17
Caprinula doublieri		
91 Composite Carbonate Section, Portugal	93.45	93.17
	93.45	93.17
Caprinuloidea multitubifera		
18-Shell No. 1 Chapman Core, Texas	104.61	104.59
117 Pioneer No. 1 Schroeder, Bee Co. TX	105.81	105.36
	105.81	104.59
Caprinuloidea perfecta		
18-Shell No. 1 Chapman Core, Texas	105.88	104.12
Lampazos, Sonora Section	106.00	103.92
96 4898 # 2, Chandeleur Sound, Louisiana	105.99	105.99
117 Pioneer No. 1 Schroeder, Bee Co. TX	107.43	104.10
	107.43	103.92
Coalcomana ramosa		
89 Stanolind #1 Schmidt, Guadalupe Co. TX	112.01	111.70
Mural Composite of Sonora Sections	111.52	108.19
	112.01	108.19
Distefanella lombricalis		
66 Jebel Areif El Naqa, Sinai, Egypt	90.32	89.99
	90.32	89.99
Durania arnaudi		
101 Font Blanc, France	93.33	92.92
110 Gabal Yelleg, North Sinai	91.62	91.25
91 Composite Carbonate Section, Portugal	93.45	93.07
	93.45	91.25
Durania austinensis		
UPK 1-Austin Chalk, Austin, Texas	82.53	82.27
	82.53	82.27
Durania cornupastoris		
UPK 1 Austin Chalk, Austin, Texas	91.90	91.64
	91.90	91.64
Durania gaensis		
66 Jebel Areif El Naqa, Sinai, Egypt	90.32	89.99
	90.32	89.99

Appendix 2. Continued.

Eoradiolites davidsoni		
18-Shell No. 1 Chapman Core, Texas	106.19	104.02
19-Shell No. 1 Tomasek Core, Texas	106.86	104.00
21-Austin, Texas Composite Section	104.00	104.00
21B Colorado River Composited Section, TX	104.14	104.14
Pecos River Comp. Std. Section, TX	100.78	97.91
	106.86	97.91
Eoradiolites lyratus		
22-Nahr Ibrahim, Lebanon,	104.24	102.22
47-Wadi Mi'aidin, Oman, Philip	96.07	93.83
400 Wadi Bani Kharus, Oman	101.21	101.21
406 Wadi El Assyi, Oman	104.66	104.66
109 Gabal El Minsherah, North Sinai	94.00	93.66
110 Gabal Yelleg, North Sinai	94.50	93.74
67 Gebel Abu Zurub, Sinai, Egypt	94.55	94.55
	104.24	93.74
Glossomyophorus sp.		
75 North Huqf, Oman, section S 001	122.85	122.42
76 North Huqf, Oman, section S 008	122.99	122.96
	122.99	122.42
Hippurites requieni		
MIDK 101 Font Blanc, France	92.70	92.53
66 Jebel Areif El Naqa, Sinai, Egypt	91.08	89.99
67 Gebel Abu Zurub, Sinai, Egypt	91.09	91.05
68 Gebel Guna, Sinai, Egypt	91.64	91.59
	92.70	89.99
Horiopleura baylei		
80 Sierra del Carche Prebetic, Spain	120.61	116.34
	120.61	116.34
Horiopleura lamberti		
80 Sierra del Carche Prebetic, Spain	115.57	112.06
	115.57	112.06
Ichthyosarcolites bicarinatus		
73 Cres Island, Croatia	95.95	94.22
	95.95	94.22
Ichthyosarcolites poljaki		
73 Cres Island, Croatia	95.95	94.22
	95.95	94.22
Ichthyosarcolites tricarinatus		
73 Cres Island, Croatia section	95.95	94.22
	95.95	94.22

Appendix 2. Continued.

Kimbleia albrittoni
  Pecos River Comp. Std. Section, TX   100.23   97.91
  96 4898 # 2, Chandeleur Sound, Louisiana   98.13   97.91
                                                              _____   _____
                                                              100.23   97.91

Kimbleia capacis
  Pecos River Comp. Std. Section, TX   100.27   98.23
                                                              _____   _____
                                                              100.27   98.23

Mexicaprina alata
  96 4898 # 2, Chandeleur Sound, Louisiana   98.09   97.97
                                                              _____   _____
                                                              98.09   97.97

Mexicaprina cornuta
  Pecos River Comp. Std. Section, TX   99.64   99.14
                                                              _____   _____
                                                              99.64   99.14

Mexicaprina minuta
  Pecos River Comp. Std. Section, TX   98.75   97.91
                                                              _____   _____
                                                              98.75   97.91

Mexicaprina quadrata
  96 4898 # 2, Chandeleur Sound, Louisiana   98.14   97.91
                                                              _____   _____
                                                              98.14   97.91

Monopleura marcida
  21B Colorado River Composited Section Re   105.53   105.50
  85 Blanco River, TX Composited Section   105.53   105.49
  89 Stanolind #1 Schmidt, Guadalupe Co. TX   111.69   109.01
                                                              _____   _____
                                                              111.69   105.49

Offneria sp.
  76 North Huqf, Oman, section S 008   122.70   122.67
  80 Sierra del Carche Prebetic zone, Spain   122.03   120.72
                                                              _____   _____
                                                              122.70   120.72

Orthopthychus striatus
  73 Cres Island, Croatia section   95.95   94.22
                                                              _____   _____
                                                              95.95   94.22

Pachytraga paradoxa
  80 Sierra del Carche Prebetic zone, Spain   122.03   120.72
                                                              _____   _____
                                                              122.03   120.72

Petalodontia calamitiformis
  18-Shell No. 1 Chapman Core, Texas   105.84   104.05
  19-Shell No. 1 Tomasek Core, Texas   106.82   104.04
  MIDK 117 Pioneer No. 1 Schroeder, Bee Co   105.88   104.95
                                                              _____   _____
                                                              106.82   104.04

Appendix 2. Continued.

Polyconites verneuilli

80 Sierra del Carche Prebetic zone, Spain	115.57	112.06
	115.57	112.06

Praeradiolites biskraensis

MIDK 109 Gabal El Minsherah, North Sinai	93.96	93.96
	93.96	93.96

Praeradiolites fleuriaui

67 Gebel Abu Zurub, Sinai, Egypt	91.63	91.63
	91.63	91.63

Praeradiolites irregularis

22-Nahr Ibrahim, Lebanon, Alb-Cen	92.99	92.51
47-Wadi Mi'aidin, Oman, Philip	***	91.75
	92.99	92.75

Praeradiolites sp.

16-Wadi Miaidin, Oman, Scott, 1990	98.16	91.75
47-Wadi Mi'aidin, Oman, Philip	91.75	***
16B Wadi Miaidin, Oman (Scott, 1990)	98.15	94.58
	98.16	94.06

Pseudotoucasia santanderensis

80 Sierra del Carche Prebetic zone, Spain	114.91	113.71
	114.91	113.71

Radiolites lusitanicus

91 Composite Carbonate Section, S. Portugal	93.23	93.06
	93.23	93.06

Radiolites peroni

91 Composite Carbonate Section, S. Portugal	93.06	93.06
	93.06	93.06

Radiolites sauvagesi

66 Jebel Areif El Naqa, Sinai, Egypt	90.32	89.99
	90.32	89.99

Sauvagesia sharpei

MIDK 101 Font Blanc, France	93.33	93.17
91 Composite Carbonate Section, Portugal	93.45	93.13
	93.45	93.13

Sauvagesia sp.

47-Wadi Mi'aidin, Oman, Philip	91.60	91.52
	91.60	91.52

Sauvagesia acutocostata

UPK 1-Austin Chalk, Austin, Texas	82.53	82.27
	82.53	82.27

Appendix 2. Continued.

Schiosia carinatoformis		
73 Cres Island, Croatia	95.95	94.22
	95.95	94.22
Sphaerulites sp.		
47-Wadi Mi'aidin, Oman, Philip, 1993	96.07	94.42
	96.07	94.42
Texicaprina vivari		
18-Shell No. 1 Chapman Core, Texas	105.88	104.05
19-Shell No. 1 Tomasek Core, Texas	107.37	103.92
21-Austin, Texas Composite Section	104.03	103.94
Pecos River Comp. Std. Section, TX	100.29	100.29
Lampazos, Sonora Section	106.00	103.92
21B Colorado River Composited Section Re	105.53	105.50
117 Pioneer No. 1 Schroeder, Bee Co. TX	105.36	104.75
	107.37	100.29
Toucasia patagiata		
21B Colorado River Composited Section	105.53	105.50
85 Blanco River, TX Composited Section	105.53	105.49
	105.53	105.49
Toucasia texana		
18-Shell No. 1 Chapman Core, Texas	105.16	104.02
19-Shell No. 1 Tomasek Core, Texas	104.34	103.92
21-Austin, Texas Composite Section	104.03	103.94
	105.16	103.92
Vaccinites praegiganteus		
UPK 38 Section 1, Bey Dağları, Turkey	91.47	91.14
	91.47	91.14